Biochemical Pharmacology 80 (2010) 236–246

Contents lists available at ScienceDirect

Biochemical Pharmacology

journal homepage: www.elsevier.com/locate/biochempharm

Extracellular calcium-sensing receptor mediates human bronchial epithelial wound repair

Javier Milara [a,*], Manuel Mata [a], Adela Serrano [a], Teresa Peiró [a], Esteban J. Morcillo [b,c,d], Julio Cortijo [a,b,c]

[a] Research Unit, University General Hospital Consortium, Av. Tres Cruces s/n E-46014 Valencia, Spain
[b] Department of Pharmacology, Faculty of Medicine, University of Valencia, Av. Blasco Ibanez 17, E-46010 Valencia, Spain
[c] CIBERES, Health Institute Carlos III, Valencia, Spain
[d] Clinical Pharmacology Unit, University Clinic Hospital, Av. Blasco Ibanez 17, E-46010 Valencia, Spain

ARTICLE INFO

Article history:
Received 27 January 2010
Accepted 30 March 2010

Keywords:
Calcium-sensing receptor
Airway epithelial wound repair
Migration
Proliferation

ABSTRACT

The airway epithelium routinely undergoes damage that requires repair to restore epithelial barrier integrity. Cell migration followed by proliferation are necessary steps to achieve epithelial repair. Calcium-sensing receptor (CaSR) is implicated in cell migration and proliferation processes. Thus we hypothesized that CaSR mediates lung epithelial wound repair. We detected CaSR expression in human lung and in well-differentiated human bronchial epithelial cells (HBEC). To test the CaSR functionality, HBEC loaded with fura-2 were stimulated with extracellular Ca^{2+} ($[Ca^{2+}]_{out}$) which resulted in a concentration-dependent intracellular Ca^{2+} ($[Ca^{2+}]_i$) increase (potency ~ 5.6 mM $[Ca^{2+}]_{out}$). Furthermore, increasing $[Ca^{2+}]_{out}$ induced phosphorylation of the extracellular signal-regulated kinase (ERK1/2) which was blocked by siRNA-CaSR and the specific inhibitor of CaSR, NPS2390.

Epithelial repair after mechanical injury of differentiated HBEC was a process dependent of $[Ca^{2+}]_{out}$ since it accelerated wound repair and HBEC proliferation being highest at 5 mM $[Ca^{2+}]_{out}$. Furthermore, U73122 (an inhibitor of phospholipase C (PLC)) and PD 98059 (an inhibitor of ERK1/2) as well as siRNA-CaSR and NPS2390 partially inhibited wound repair and HBEC proliferation. On the other hand, mechanical injury produced an $[Ca^{2+}]_i$ wave propagation that was partially inhibited by siRNA-CaSR, NPS2390 and the extracellular Ca^{2+} chelator EGTA, which suggest a link of CaSR between cell–cell communication and wound repair in differentiated HBEC. Our data, for the first time, shows that CaSR plays an important role in airway epithelial repair, which may help to develop novel regenerative therapeutics allowing the rapid repair of lung damaged epithelium.

1. Introduction

The airway epithelium acts as a protective barrier preventing the exposure of the underlying tissue to noxious particles. The epithelium is routinely challenged by allergens and inhaled air pollutants, resulting in a damage that requires repair to restore barrier integrity. Damage is also commonly seen in diseases such as asthma or chronic obstructive pulmonary disease (COPD) among others [1,2]. Furthermore, the epithelium is not only a passive barrier, but also a source of inflammatory cytokines [2].

The mechanisms and regulators of epithelial repair are poorly understood. In this process a common sequence of injury and wound repair have been described *in vivo* [2]. The first step in epithelial repair is the migration of the basal cells neighboring the wound, followed by proliferation and active mitosis and squamous metaplasia. Finally, progressive redifferentiation with the emergence of preciliated cells (mixed phenotype of ciliated cells with mucous secretory granules) followed by ciliogenesis and complete regeneration of a pseudostratified mucociliary epithelium complete epithelial repair [3]. Numerous cellular and molecular factors are involved in the repair and regeneration of the airway epithelium. These factors are modulated by the matrix metalloproteinases (MMPs), cytokines, and growth factors released by the epithelial and mesenchymal cells [2].

In the initial damage subsequent to an inflammatory context, epithelial cells may communicate with each other through the fast propagation of intracellular Ca^{2+} waves helping neighbouring cells to induce migration and proliferation in order to wounding repair [4,5]. Among the factors and mechanisms that produce Ca^{2+} waves after airway epithelial injury, extracellular Ca^{2+} ($[Ca^{2+}]_{out}$), and

* Corresponding author at: Unidad de Investigación, Consorcio Hospital General Universitario, Avenida Tres Cruces s/n, E-46014 Valencia, Spain.
Tel.: +34 620231549, fax: +34 961972145.
E-mail addresses: xmilara@hotmail.com (J. Milara), manuel.mata@uv.es (M. Mata), adela_serrano@hotmail.com (A. Serrano), tepeisal@alumni.uv.es (T. Peiró), Esteban.Morcillo@uv.es (E.J. Morcillo), julio.cortijo@uv.es (J. Cortijo).

0006-2952/$ – see front matter © 2010 Elsevier Inc. All rights reserved.
doi:10.1016/j.bcp.2010.03.035

intracellular Ca^{2+} ($[Ca^{2+}]_i$) play a key role in these orchestrating communications [4–6].

It is well established in several cell types that the majority of Ca^{2+} released during intracellular signalling events is exported to the extracellular space, usually through the activity of the plasma membrane Ca^{2+} ATPase [7,8]. As internal Ca^{2+} stores maintain a total $[Ca^{2+}]$ of several mM [9], and the ratio of extracellular space volume to cell volume is very small in a structurally intact tissue, substantial fluctuations in $[Ca^{2+}]_{out}$ are expected to occur as a consequence.

Cell-surface proteins that can act as sensors of $[Ca^{2+}]_{out}$, have been observed in a number of biological systems. In particular, calcium-sensing receptor (CaSR) has been implicated as an important factor mediating the propagation of intercellular signals between cells [10]. CaSR was originally cloned from the parathyroid gland, but now it is known that it is expressed in a wide variety of mammalian tissues and cell types although its function remains to be elucidated [11]. The CaSR is cooperatively activated by Ca^{2+} ions over a concentration range of 0.5–10 mM resulting in a cell-type-specific coupling to intracellular signalling cascades such as phospholipase C (PLC)/$InsP_3$/Ca^{2+}, adenosine 3′,5′-cyclic monophosphate (cAMP) and MAP-kinase pathways [12]. CaSR has been identified in rat lung [13], and recently we have observed that nickel triggers intracellular Ca^{2+} mobilization and inflammatory mediators in human airway epithelial cells through the activation of CaSR [14], however its physiological role in human airway epithelium remains unclear.

Since CaSR mediates cell–cell communications through $[Ca^{2+}]_{out}$ local levels, we hypothesized that the expression of CaSR on human bronchial epithelial cells (HBEC) may be related with epithelial repair. We found that the lack of expression or the inhibition of the CaSR may delay the process of airway epithelial wound repair in well-differentiated HBEC cultures which may contribute to the understanding of airway epithelial repair following lung injury.

2. Materials and methods

Unless otherwise stated, all reagents used were obtained from Sigma (Chemical Co., Madrid, Spain). U73122, NPS 2390, PD 98059, BAPTA-acetoxymethyl ester (AM) and Fura-2AM were disolved in dimethyl sulfoxide (DMSO) at 10 mM stock concentration. Several dilutions of the stocks were performed with cell culture medium. The final concentration of DMSO in the culture cell did not exceed 0.1% and had no significant pharmacological activity.

2.1. Cell culture

Human lung tissue was obtained from patients who were undergoing surgery for lung carcinoma: with local ethic committee approval; informed consent was obtained. To discard lung tumour influence on CaSR expression, healthy lung tissue from a patient who died in a car accident was included previous informed consent of the family. Primary cultures of HBEC were obtained from human lung tissue as previously outlined [15]. HBEC monolayers were grown in basal airway epithelial growth media (BEGM, Clonetics, UK). To differentiate airway epithelium, HBEC were cultured and differentiated in transwell inserts (Corning Costar, Buckinghamshire, UK) under an air–liquid interface (ALI) as previously described [14]. Briefly, a multilayered bronchial epithelium was produced by seeding cells (8.25×10^4 cells/insert) onto polyester inserts. They were submerged in differentiation media (50% DMEM (Clonetics, UK) in basal airway epithelial growth media (BEGM, Clonetics, UK) for the first 7 days. Cells were then cultured during 21 additional days with the apical surface exposed to air. Throughout the culture period, cells were maintained at 37 °C in a 5% CO_2 incubator with media changes every 48 h.

2.2. Intracellular free Ca^{2+} measurements

$[Ca^{2+}]_i$ was measured by epifluorescence microscopy (Nikon eclipse TE200 inverted microscope, Tokyo, Japan) in cultured HBEC monolayers or in differentiated HBEC in ALI using the Ca^{2+} indicator dye fura-2AM as previously outlined [14,16]. Both, HBEC monolayers and differentiated HBEC Ca^{2+} experiments were done in Hank's balanced salt solution (HBSS, Clonetics, UK) without phenol red. In brief, fluorescence of fura-2AM (5 μM)-loaded cells was measured by using continuous rapid alternating excitation (340 and 380 nm) and emission (510 nm) in a fluorescence spectrophotometer equipped with a xenon lamp (Nikon XB0 100, Tokyo, Japan) and a CDD camera CoolSNAPfx (photometrics, Tokyo, Japan) (20 MHz, 1300 × 1030 pixel). The fluorescence ratio was recorded every 3 s using Lambda 10-2 Sutter Instrument (Nikon Co., Tokyo, Japan) and fluorescence analysis was performed with the software Metafluor® 5.0 (Molecular Devices, USA). A baseline was established for 15 s. Data are presented as changes in fluorescence ratio F_{340}/F_{380} intensities compared with baseline values. Intracellular Ca^{2+} wave propagation after mechanical injury in differentiated HBEC in ALI cultures were performed as previously reported with modifications [17]. In brief, transwell inserts were immersed in HBSS and fixed to the bottom in a 6-well plate. Wounds were made in differentiated HBEC by scratching by micromanipulator (Narishige, USA) with a fresh 18 G needle (tip diameter, 8 μm) which removed cells from about 100–200 μm. Differentiated HBEC were observed on the inverted epifluorescence microscopy during the fluorescence imaging ratio with a nikon CF fluor ×40 objective. To be sure that the wound was always made in the same relative position the needle was located initially in the upper right field of the fluorescence image. In these experiments we monitored fluorescence ratio F_{340}/F_{380} intensities simultaneously in the full fold of the image (×400 magnification) during 300 s following wound healing. Wave Ca^{2+} propagation was considered as the duration of time of the maximal fluorescence intensity observed in the full fold image. Calcium peak intensity was observed when calcium wave occupied the full fold image. Calcium wave was correlated with the area under curve of the fluorescence intensity around the total time (300 s) of the experiment.

2.3. Wound repair studies

Differentiated HBEC repair studies were carried out in 12-well transwell inserts in antibiotic free #CnT-23BM differentiated culture media with supplements CnT-23S (CELLNTEC, Switzerland) without Ca^{2+}. The different requirements of $[Ca^{2+}]_{out}$ were added in each concrete experiment. Wound closure assay on differentiated HBEC showed an *in vitro* approximation of the real *in vivo* conditions as previously outlined [18]. Differentiated HBEC were pre-treated with pharmacologic modulators for 30 min and scrape-wounded using a sterile p200 pipette tip by one perpendicular linear scratch, creating a wound of 4 1 mm width across the diameter of the insert. Transwell inserts were then washed two times with the same differentiated medium to eliminate floating and dead cells. After washing, differentiation culture media was added with or without pharmacologic modulators or with different $[Ca^{2+}]_{out}$. To be sure that the wound area measures were done in the same place during wound closure, a black line was painted to the bottom of each plate and wound areas were measured in the intersection of the wound and the black line. Wound closure was monitored immediately after initial wounding using a 5× phase contrast objective lens and was digitally captured at regular time intervals after wounding until repair was complete. Wound areas were analysed using Image J 1.42q software (available at: http://rsb.info.nih.gov/ij/, USA); the extent of repair was calculated and expressed as a percentage of the original wound area.

2.4. Proliferation assay

HBEC cell proliferation was measured by colorimetric immunoassay based on BrdU incorporation during DNA synthesis using a cell proliferation enzyme-linked immunosorbent assay BrdU kit (Roche, Mannheim, Germany) according to the manufacturer's protocol as previously outlined [14]. Semiconfluent cultured HBEC were grown in 96-well plates at a density of 3×10^3 cells/well and incubated for 24 h in antibiotic free #CnT-17BM airway epithelial culture media with supplements CnT-17S (CELLNTEC, Switzerland) without Ca^{2+}. The different requirements of $[Ca^{2+}]_{out}$ were added in each concrete experiment. Cells were then exposed to different $[Ca^{2+}]_{out}$ for 24 h. The different pharmacologic modulators were added to the cells 1 h before addition of $[Ca^{2+}]_{out}$. The 490 nm absorbance was quantified using a microplate spectrophotometer (Victor 1420 Multilabel Counter, PerkinElmer). Proliferation data refer to the absorbance values of BrdU-labeled cellular DNA content per well. Stimulation is expressed as *x*-fold proliferation over basal growth of the untreated control (0 mM Ca^{2+} basal #CnT-17BM plus CnT-17S) set as unity.

2.5. Western blot

Western blot analysis was used to detect CaSR protein (150–135 kDa), phospho-ERK 1/2 and total ERK 1/2 (42–44 kDa) proteins in differentiated HBEC. Cells were scraped from well differentiated HBEC and lysed on ice with a lysis buffer consisting of a complete inhibitor cocktail plus 1 mM ethylenediaminetetraacectic acid (Roche Diagnostics Ltd., West Sussex, UK) with 20 mM Tris base, 0.9% NaCl, 0.1% Triton X-100, 1 mM dithiothreitol, and 1 $\mu g\ ml^{-1}$ pepstatin A. The Bio-Rad assay (Bio-Rad Laboratories Ltd., Herts, UK) was used (following manufacturer's instructions) to quantify the level of protein in each sample to ensure equal protein loading. Sodium dodecyl sulphate polyacrylamide gel electrophoresis was used to separate the proteins according to their molecular weight. Briefly, 20 μg proteins (denatured) along with a molecular weight protein marker, Bio-Rad Kaleidoscope marker (Bio-Rad Laboratories Ltd., Herts, UK), were loaded onto an acrylamide gel consisting of a 5% acrylamide stacking gel stacked on top of a 10% acrylamide resolving gel and run through the gel by application of 100 V for 1 h. Proteins were transferred from the gel to a polyvinylidene difluoride membrane using a wet blotting method. The membrane was blocked with 5% Marvel in PBS containing 0.1% Tween20 (PBS-T) and then probed with the following antibodies: anti-CaSR (1:1000) antibody (mouse polyclonal antibody, cat no. MA1–934, Affinity Bioreagents, UK), anti-CaSR (1:1000) antibody (mouse monoclonal antibody, cat no. C0493, Sigma), with anti-p-ERK 1/2 (1:1000, cat no. 4376S, Cell signalling, USA) and ERK 1/2 (1:1000, cat no. 4695, Cell signalling, USA) or with β-actin (1:1000, Sigma, Spain) as internal control, followed by a peroxidase conjugated secondary (1:10,000) antibody. The enhanced chemiluminescence method of protein detection using enhanced chemiluminescence reagents (Amersham GE Healthcare, Buckinghamshire, UK) was used to detect labelled proteins.

2.6. Immunohistochemistry and immunofluorescence

Human lung tissue and differentiated HBEC grown in ALI cultures were fixated (4% paraformaldehyde, 30 min, room temperature). Paraffin inclusion and sections were performed as outlined [14]. Briefly, slices were permeabilized (20 mM HEPES, pH 7.6, 300 mM sucrose, 50 mM NaCl, 3 mM $MgCl_2$, 0.5% Triton X-100), blocked (10% goat serum in PBS), and incubated with the primary antibody (anti-human CaSR mAb, 1:1000; MA1–934 and C0493) overnight at 4 °C followed by secondary antibody anti-mouse rhodamine 1:100 and DAPI (2 μg/ml) to mark nuclei (Molecular Probes, Leiden, The Netherlands) for immunofluorescence, or secondary anti-rabbit antibody (1:100; Vector Laboratories, Burlingame, CA) with avidin–biotin complex/horseradish peroxidase (for 30 min) for immunohistochemistry. Tissue was counterstained with hematoxylin. Slices were visualized by epifluorescence microscopy (×200; Nikon eclipse TE200 inverted microscope, Tokyo, Japan).

In other experiments, HBEC were grown in monolayers or were differentiated in ALI before fixation (4% paraformaldehyde, 30 min, at room temperature). HBEC on coverslips (for monolayer cell cultures) (22 mm #1.5, Dow Corning, Midland, MI) or differentiated HBEC on polyester inserts were treated with the anti-human CaSR mAb, 1:1000; polyclonal MA1–934 and monoclonal C0493, and a secondary anti-mouse antibody labelled with FITC or rhodamine (1:100, Molecular Probes, UK). The specificity of the immunostaining was confirmed by the substitution of primary antibody with an irrelevant IgG1 mouse and by omission of the primary antibody. No positive immunostaining was observed in IgG1 anti-mouse control in slice tissues and HBEC preparations.

2.7. Transfection of CaSR siRNA

In non-differentiated HBEC, small interfering RNA (siRNA) was transfected with CaSR-targeted siRNA (Ambion, Austin TX, USA. PN 4392420) or negative control scramble (−) siRNA with no homology to the human genome (Ambion, Huntingdon, Cambridge, UK) at concentration of 50 nM in serum free medium over a period of 6 h, the medium was then aspirated and replaced with serum containing medium for a further period of 42 h before proliferation experiments. The transfection reagent used in non-differentiated HBEC monolayer was lipofectamine-2000 (Invitrogen, Paisley, UK) at a final concentration of 2 μl/ml.

In differentiated HBEC, siRNA transfection was performed with commercial siRNA against CaSR (Ambion, Austin TX, USA; PN 4392420) or with 50 nM siRNA control (Ambion, Huntingdon, Cambridge, UK), through reverse permeabilization technique as previously outlined [19]. In other experiments, differentiated HBEC were transfected with Silencer® Cy™3 labeled Negative Control #1 siRNA; PN AM4621) to verify the internalization of the siRNA inside cells. Briefly, differentiated HBEC were exposed to three successive solutions (4 °C) containing (in mM): (1) 10 EGTA, 120 KCl, 5 ATP, 2 $MgCl_2$, 20 TES (pH 6.8; 20 min); (2) 120 KCl, 5 ATP, 2 $MgCl_2$, 20 TES and 50 nM siRNA (pH 6.8; 3 h); and (3) 120 KCl, 5 ATP, 10 $MgCl_2$, 20 TES and 50 nM siRNA (pH 6.8; 30 min). Subsequently, ALI epithelial cells were bathed in a fourth solution containing (in mM) 140 NaCl, 5 KCl, 10 $MgCl_2$, 5 glucose, and 2 MOPS (pH 7.1, 22 °C) in which Ca^{2+} concentration was gradually increased from 0.01 to 0.1 to 1.8 mM every 15 min. Then, cells were cultured in differentiation media. The protein expression for CaSR was monitored for 48, 72 and 96 h by Western blot to determine silencing efficiency.

2.8. Statistics

Data are presented as mean ± SEM of *n* experiments. Statistical analysis of data was carried out by analysis of variance (ANOVA) followed by Bonferroni test (GraphPad Software Inc., San Diego, CA, USA). Significance was accepted when $P < 0.05$.

3. Results

3.1. CaSR is expressed in human lung tissue

CaSR protein expression was detected in the human lung, mainly in epithelial cells from human bronchus (Fig. 1, panels a–d, representative of four patients).

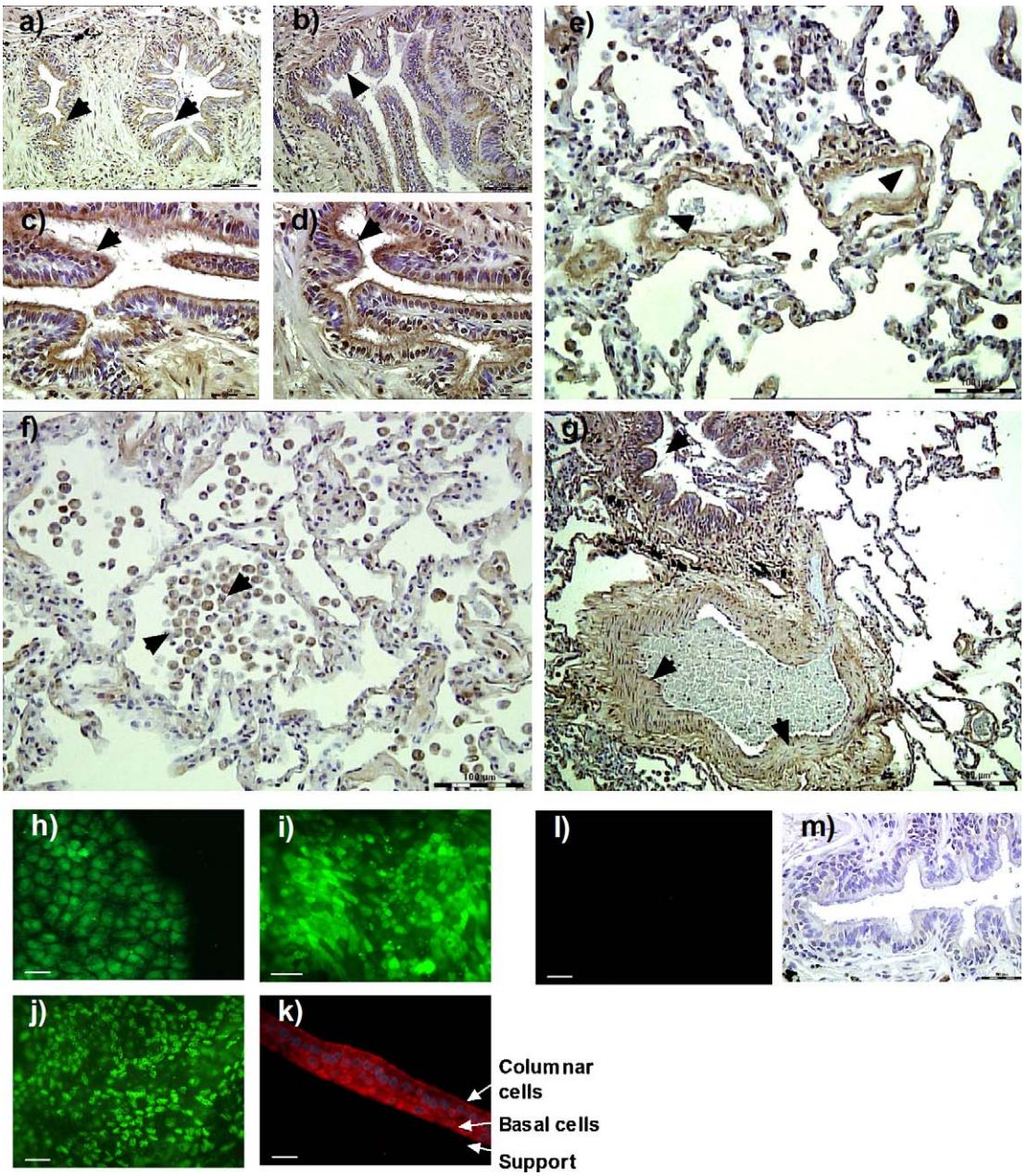

Fig. 1. Expression of CaSR in lung tissue. Photomicrographs of representative histological sections from human lung tissue of four different patients, from bronchus (panels a–d represent four sections of four different patients), pulmonary veins (panel e), parenchyma and alveolar macrophages (panel f) or pulmonary artery with bronchus (panel g). Slice tissue sections were immunostaining against CaSR with MA1–934 and C0493 antibodies. Representative sections are shown to CaSR MA1–934 antibody. Tissue was counterstained with hematoxylin (blue colour structures). Black arrows show positive immunoreactivity as brown staining. Human bronchial epithelial cells (HBEC) were grown in monolayer in 22 mm cover slips (panel h) or in transwell inserts in air liquid interface for 28 days (panels i and j) and immunostained for CaSR MA1–934 and C0493 antibodies following antimouse-FITC secondary antibody. At 28th day of HBEC differentiation CaSR was located abundantly on non-ciliated and ciliated epithelial cells (panels i and j respectively). Representative sections are shown to CaSR MA1–934 antibody. CaSR was present in basal and columnar cells in cross sections of differentiated HBEC included in paraffin (panel k). Blue color represents DAPI marked nucleus, and red color represents CaSR immunostaining. IgG1 isotype controls are shown for immunofluorescence and immunohistochemistry (panels l and m). Scale bar: 10 μm (panel h); 20 μm (panels i–l).

The CaSR pattern of expression found in healthy lung tissue (Fig. 1b) corresponded with those patients with lung carcinoma suggesting that CaSR expression was not exclusively induced by tumour microenvironment. The ontogeny was similar when any of the two antibodies defined in Section 2 were employed. For brevity, only the data using MA1–934 are presented in the text. Apart from human bronchus, CaSR was detected on smooth muscle layer from pulmonary veins (Fig. 1, panel e), alveolar macrophages (Fig. 1, panel f) and pulmonary arteries (Fig. 1, panel g). On the other hand, CaSR expression became apparent also in non-differentiated HBEC in culture (Fig. 1, panel h) as well as in differentiated HBEC in ALI (Fig. 1, panels i–k). Furthermore CaSR expression was located in almost every cell type in the pseudostratified epithelium as ciliary epithelial cells and columnar and basal human epithelial cells (Fig. 1, panels i–k) being distributed on the plasmatic membrane.

3.2. CaSR agonists evoke an increase in intracellular Ca^{2+} signalling in HBEC

In most cell types studied to date [11] activation of the G protein-coupled CaSR by its agonists causes PLC-evoked $[Ca^{2+}]_i$

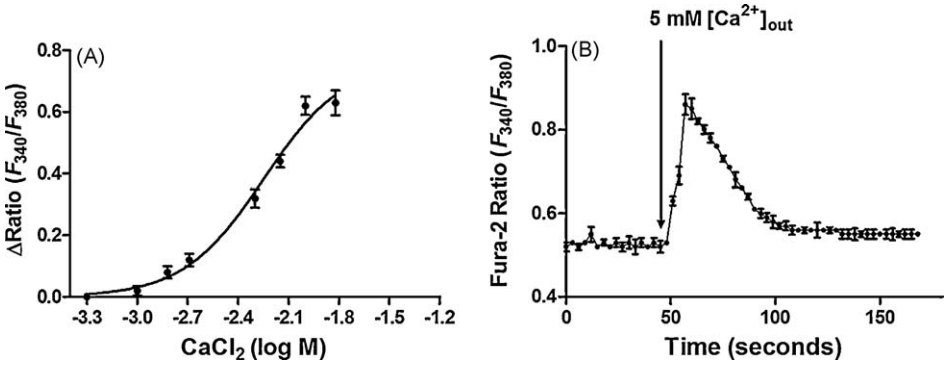

Fig. 2. Extracellular Ca^{2+} induces an intracellular Ca^{2+} transient in HBEC. (A) Concentration-dependent increase by $CaCl_2$ of the intracellular free Ca^{2+} concentration ($[Ca^{2+}]_i$) in HBEC cultured in monolayer in absence of extracellular free Ca^{2+} medium ($[Ca^{2+}]_{out}$). Changes in $[Ca^{2+}]_i$ were monitored in fura 2-AM loaded cells as described in Section 2, and results were expressed as increments of the ratio between fura 2 fluorescence intensities at 340 nm and 380 nm (F_{340}/F_{380}) with respect to basal levels of F_{340}/F_{380} ratio. (B) $CaCl_2$ (5 mM) triggered a rapid increase of fura 2 F_{340}/F_{380} ratio followed by decay to baseline in monolayer HBEC in absence of extracellular free Ca^{2+} medium. Experiments are the mean ± SEM of $n = 4$ experiments per condition.

release from internal stores as we showed previously in human airway epithelial cells stimulated with nickel [14]. To test the hypothesis that the CaSR is functional on HBEC in response to $[Ca^{2+}]_{out}$ we stimulated HBEC monolayer with different amounts of $[Ca^{2+}]_{out}$. We detected an increase in $[Ca^{2+}]_i$ in a range of 1.5–15 mM of $[Ca^{2+}]_{out}$ with a potency of ~5.6 mM (Fig. 2A; $-\log EC_{50} = 2.24 \pm 0.03$; $n = 4$). The Ca^{2+}-induced increase of $[Ca^{2+}]_i$ consisted of an initially rapid increase of $[Ca^{2+}]_i$ to reach a peak in ~15 s followed by a subsequent decline that reached a plateau baseline after ~50 s (Fig. 2B).

3.3. Repair of bronchial epithelium is dependent on $[Ca^{2+}]_{out}$-induced migration and CaSR activation

Previous studies have suggested that $[Ca^{2+}]_{out}$ signalling plays an important role during migration of a variety of cell types [20,21]. We therefore hypothesized that HBEC wound repair was likely to be a $[Ca^{2+}]_{out}$-dependent process. Fig. 3A shows the acceleration of differentiated HBEC wound repair by increasing $[Ca^{2+}]_{out}$, being maximum at 5 mM. This effect was supported by the selective extracellular $[Ca^{2+}]$ chelation with EGTA 1 mM which results in a delayed wound repair (Fig. 3B). Furthermore, $[Ca^{2+}]_i$ was critical to wound repair since selective $[Ca^{2+}]_i$ chelation with BAPTA-AM dramatically inhibited differentiated HBEC wound closure (Fig. 3B). When $[Ca^{2+}]_{out}$ and $[Ca^{2+}]_i$ were simultaneously removed with EGTA and BAPTA-AM wounding repair was completely blocked suggesting that wounding repair is totally dependent of calcium signalling (Fig. 3B). To be sure that these effects were mediated by $[Ca^{2+}]$ suppression and not by cytotoxicity of the chemical reagents, differentiated HBEC ALI cultures or monolayer cultures were incubated with 1 mM EGTA, 100 μM BAPTA-AM or their combinations for 48 h. No significant difference in the lactate dehydrogenase supernatant level (lactate dehydrogenase cytotoxicity assay; Cayman, Spain) respect control conditions were observed which discard cytotoxicity (data not shown).

On the other hand, in presence of 2.5 mM $[Ca^{2+}]_{out}$, the addition of U73122 10 μM (an inhibitor of PLC) and PD98059 10 μM (an inhibitor of ERK1/2) partially suppress wound repair suggesting the involvement of PLC and ERK1/2 pathways in $[Ca^{2+}]_{out}$-induced wound closure of differentiated HBEC.

Since $[Ca^{2+}]_{out}$ may activate $[Ca^{2+}]_i$ and PLC/ERK1/2 through the G protein-coupled receptor CaSR [12], we investigated the role of the CaSR antagonism in wound repair. NPS2390 has been employed previously as CaSR antagonist in a range of 1–10 μM [22–24]. In this work, we observed that NPS2390 concentration-dependently inhibited wound repair significantly at 1 and 10 μM (Fig. 3C). To further study the role of CaSR on wound repair we targeted suppressed CaSR with specific siRNA-CaSR. Thus, differentiated HBEC were reversibly permeabilizated and a fluorescence Cy™3 labeled non-selective small interfering RNA ((−)siRNA) was detected verifying the correct internalization of the siRNA inside cells (Fig. 4A). CaSR protein downregulation was detected in differentiated HBEC by Western blot following 72 h being highest at 96 h after siRNA-CaSR transfection (Fig. 4A). In this sense, scrape-wounded was performed at 96 h after siRNA-CaSR transfection which significantly inhibited wound closure (Fig. 4B).

In the process of airway epithelial damage and repair different cell types are involved. Thus, basal cells migrate neighbouring the wound, squamous cells are transient epithelial cells involved in the regeneration process, while ciliated cells are representative of the complete regenerated pseudostratified mucociliary epithelium [2]. We investigated the expression of CaSR after the 24 h post-wound in differentiated HBEC. In the margins of wound, CaSR was located mainly around the cellular nucleus (Fig. 4C, panel b) showing a possible immature CaSR protein derived from the active proliferation found after 24 h post-wounding [2]. However epithelial cells located in the recently repaired area showed a global and plasmatic membrane distribution (Fig. 4C, panel c). On the other hand, in non-damaged epithelium CaSR was located abundantly on ciliated cells (Fig. 4C, panel d).

3.4. Wound causes a $[Ca^{2+}]_i$ wave in differentiated HBEC which is partially mediated by CaSR

Recently it has been shown that CaSR mediates cell–cell communication in response to $[Ca^{2+}]_{out}$ fluctuations between cells [25]. In this work we targeted suppressed CaSR with specific siRNA-CaSR during 96 h in differentiated HBEC, and then cells were loaded with fura-2 and wounded with a 18-gauge needle. Immediately after the cells were wounded, $[Ca^{2+}]_i$ waves were started as represented by the fluorescence ratio F_{340}/F_{380} (Fig. 5A). The $[Ca^{2+}]_i$ wave propagation and the intensity of F_{340}/F_{380} signal was significantly diminished in differentiated HBEC transfected with siRNA-CaSR compared to cell transfect with the (−)siRNA control (Fig. 5A and B; $P < 0.05$). To further analyze the CaSR role on $[Ca^{2+}]_i$ wave propagation, we used 10 μM NPS2390 in presence of 1.5 mM $[Ca^{2+}]_{out}$. NPS2390 addition resulted in a diminished F_{340}/F_{380} wave intensity propagation in differentiated HBEC respect non-treated cells (Fig. 5C; $P < 0.05$). Since $[Ca^{2+}]_{out}$ is responsible of the CaSR activation, we abolished $[Ca^{2+}]_{out}$ using 1 mM EGTA which significantly inhibited F_{340}/F_{380} wave intensity propagation after wound (Fig. 5D; $P < 0.05$). Furthermore the $[Ca^{2+}]_i$ chelation by BAPTA-AM fully suppresses $[Ca^{2+}]_i$ waves (Fig. 5D; $P < 0.05$).

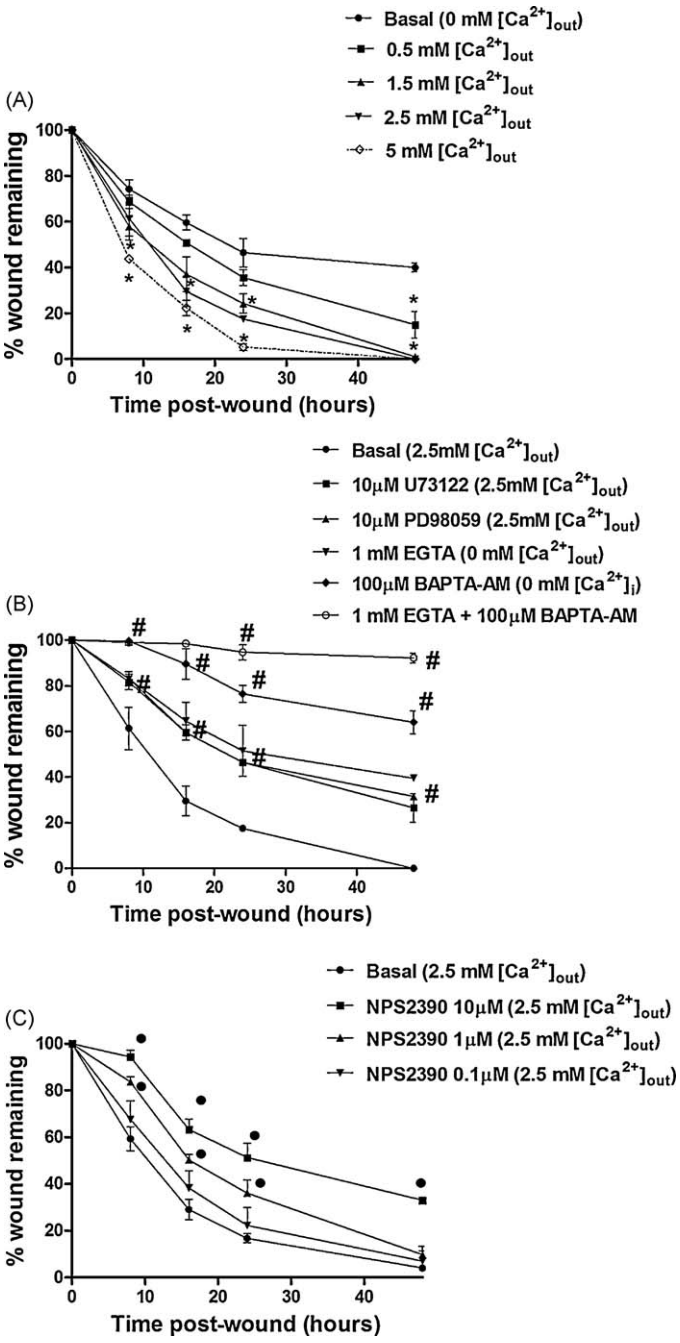

Fig. 3. Wound repair in differentiated HBEC is dependent of extracellular Ca^{2+}. (A) Differentiated HBEC wound repair is accelerated by growing extracellular Ca^{2+} concentrations reaching maximal significance at 5 mM. Note that only extracellular Ca^{2+} concentrations between 1.5 mM and 5 mM reached significance respect basal culture medium (0 mM Ca^{2+}). (B) In subsequent experiments the inhibition of phospholipase C with U71322, or the inhibition of the ERK 1/2 with PD98059 as well as the extracellular Ca^{2+} chelation (EGTA in free Ca^{2+} medium) and intracellular Ca^{2+} chelation with BAPTA-AM inhibited wound repair. (C) The inhibition of CaSR with the specific inhibitor NPS 2390 dose-dependently inhibited wound repair. Experiments are represented as mean ± SEM of the percentage of wound remaining at different times post-wound in a total of $n = 4$ per condition. $^{*}P < 0.05$ *vs* medium with 0 mM of extracellular Ca^{2+}; $^{\#}P < 0.05$ *vs* medium with 2.5 mM of extracellular Ca^{2+}; $^{\bullet}P < 0.05$ *vs* medium with 2.5 mM of extracellular Ca^{2+}.

3.5. HBEC proliferation is dependent of $[Ca^{2+}]_{out}$ and CaSR

Ca^{2+}-signalling system regulates many cellular functions as cell migration and proliferation [9]. Since cell proliferation mediates one of the steps required to wound repair we explored the effect of $[Ca^{2+}]_{out}$ and CaSR as well as its downstream pathways on HBEC proliferation. HBEC proliferation was highest between 1.5 and 2.5 mM of $[Ca^{2+}]_{out}$ culture medium and in a lesser extent at 5 mM of $[Ca^{2+}]_{out}$ with respect to HBEC exposed to 0 mM of $[Ca^{2+}]_{out}$ (Fig. 6A; $P < 0.05$ respect 0 mM of $[Ca^{2+}]_{out}$). Furthermore, suppression of $[Ca^{2+}]_i$ with BAPTA-AM inhibited HBEC proliferation below baseline (0 mM of $[Ca^{2+}]_{out}$) levels (Fig. 6A; $P < 0.05$ respect 0 mM of $[Ca^{2+}]_{out}$).

On the other hand, in presence of basal 2.5 mM of $[Ca^{2+}]_{out}$, the addition of U73122 10 μM or PD98059 10 μM partially suppresses HBEC proliferation suggesting the involvement of PLC and ERK1/2 pathways in $[Ca^{2+}]_{out}$-induced proliferation (Fig. 6B; $P < 0.05$ respect basal 2.5 mM of $[Ca^{2+}]_{out}$ condition). To test the effect of CaSR on HBEC proliferation we added NPS2390 to HBEC at different doses (0.1–10 μM). In presence of 2.5 mM of $[Ca^{2+}]_{out}$, NPS2390 significantly inhibited cell proliferation at doses of 1 and 10 μM (Fig. 6C; $P < 0.05$). In addition, non-differentiated HBEC transfected with siRNA-CaSR suppressed CaSR protein expression (Fig. 6B) which significantly reduced HBEC proliferation compared to negative control (−) siRNA (Fig. 6D; $P < 0.05$).

3.6. $[Ca^{2+}]_{out}$ activates ERK1/2 through CaSR in differentiated HBEC

CaSR-induced signalling involves $[Ca^{2+}]_i$ mobilization as well as the activation of various phospholipases and protein kinases. In this work we have observed that the activation of CaSR increases $[Ca^{2+}]_i$ in HBEC and that the use of inhibitors of PLC and ERK1/2 inhibits migration and proliferation of HBEC. Thus, in order to explore whether CaSR activation induces phosphorylation of ERK1/2, increasing $[Ca^{2+}]_{out}$ were added to differentiated HBEC. After 20 min of $[Ca^{2+}]_{out}$ stimulation phospho-ERK1/2 protein expression was increased being highest at 5 mM (Fig. 7A). Furthermore, both CaSR antagonism by NPS2390 as well as CaSR silencing by siRNA-CaSR effectively suppressed phospho-ERK1/2 protein expression induced by 5 mM of $[Ca^{2+}]_{out}$ (Fig. 7B) suggesting that phosphorylation of ERK1/2 by CaSR activation partially mediates wound repair.

4. Discussion

The present study demonstrates that CaSR is expressed in human lung tissue and that it partially mediates wound repair process in well-differentiated HBEC. The evidence of CaSR in wound repair was assessed by the use of specific inhibitor and transient siRNA-CaSR. Furthermore, we observed that CaSR mediates $[Ca^{2+}]_i$ waves after epithelial injury through local $[Ca^{2+}]_{out}$ increases inducing PLC activation, $[Ca^{2+}]_i$ elevation as well as ERK1/2 phosphorylation which in turn activates cell migration and proliferation mediating wound repair. These findings identify CaSR as a potential new receptor involved in protection of the airway epithelial barrier.

CaSR was initially cloned in the parathyroid gland [26] and its function has been extensively studied in homeostatic Ca^{2+} detection, where it senses small changes in blood $[Ca^{2+}]_{out}$ and adjusts the secretion of parathyroid hormone accordingly [11]. However, the role of CaSR in tissues uninvolved in systemic ionic homeostasis is now subject to an increasing attention. To this respect, CaSR was found along the entire gastrointestinal tract [27] in human keratinocytes [28], in nervous system [29] and in breast and ovarian epithelium among other [30]. More recently, CaSR has been discovered in the blood vessel wall where it regulates arterial tone, peripheral vascular resistance and vascular inflammation and repair [31]. Furthermore, the expression of CaSR on monocyte–macrophage has been related with its migration at sites of inflammation where $[Ca^{2+}]_{out}$ are elevated [32]. In this study we have observed a marked expression of CaSR

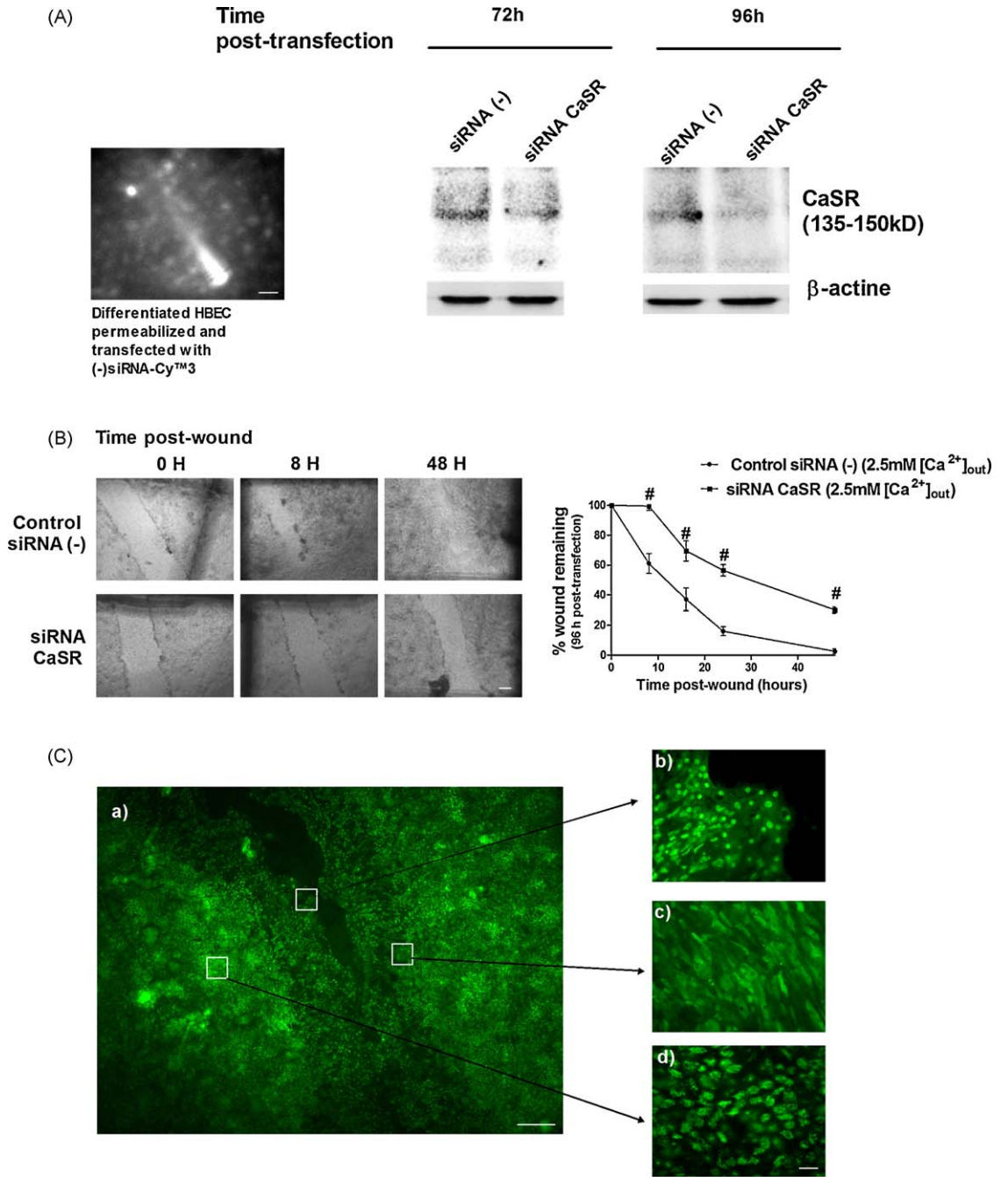

Fig. 4. Silence of CaSR in differentiated HBEC delay wound repair. (A) Differentiated HBEC were reversibly permeabilizated as described in Section 2 using a fluorescence Cy™3 labeled non-selective small interfering RNA (−)siRNA to verify the internalization of the siRNA inside cells (scale bar: 20 μm). siRNA targeted CaSR was introduced by reverse permeabilization into differentiated HBEC and the expression of CaSR protein was monitored after 72 and 96 h and compared to CaSR expression in differentiated HBEC transfected with control (−)siRNA. The expression of CaSR was reduced maximally at 92 h post-transfection. Results are representative of $n = 3$ in a total of three different siRNA transfections. (B) Differentiated HBEC wound repair is delayed when CaSR protein is downregulated by siRNA targeted CaSR. Representative phase contrast images of wound closure are showed (50× magnification) after 0, 8 and 48 h post-wound in differentiated HBEC with siRNA-CaSR or its control (−)siRNA. Experiments are represented as mean ± SEM of the percentage of wound remaining at different times post-wound in a total of $n = 3$ per condition in three different transfections. $^{\#}P < 0.05$ vs differentiated HBEC silencing with control (−) siRNA in culture medium with 2.5 mM of extracellular Ca^{2+}. (C) One linear wound was created on differentiated HBEC and after 24 h post-wound was fixed in 4% paraformaldehyde. After permeabilization differentiated HBEC were immunostained with CaSR antibody and its respective secondary antibody-FITC. Image shows the CaSR distribution across wound in a full field (panel a), in cells located at the wound border where CaSR was located mainly on the nucleus (panel b), in cells located near the border where CaSR was expressed around the complete cell (panel c), or in cells located far of the wound border where CaSR was ubiquitously expressed and detected abundantly on ciliated cells (panel d). Images are representatives of four different wounds in air liquid interface cultures of HBEC. Scale bars; 300 μm (panel a); 10 μm (panels b–d).

on pulmonary veins and arteries corroborating previous findings in non-pulmonary vascular wall [31]. Alveolar macrophages with CaSR high expression were also observed which may partially explain its migration to lung parenchyma. However the role of CaSR on pulmonary circulation remains to be elucidated. Recently, the expression of CaSR has been related with the regulation of mouse lung development [33]. In this work CaSR was expressed mainly on bronchial epithelial cells and was apparent until 18 embryonic day, after which the receptor was absent [33]. In contrast to this report we have found CaSR expression on adult bronchial epithelial cells from four different patients. Furthermore, the CaSR protein and mRNA was

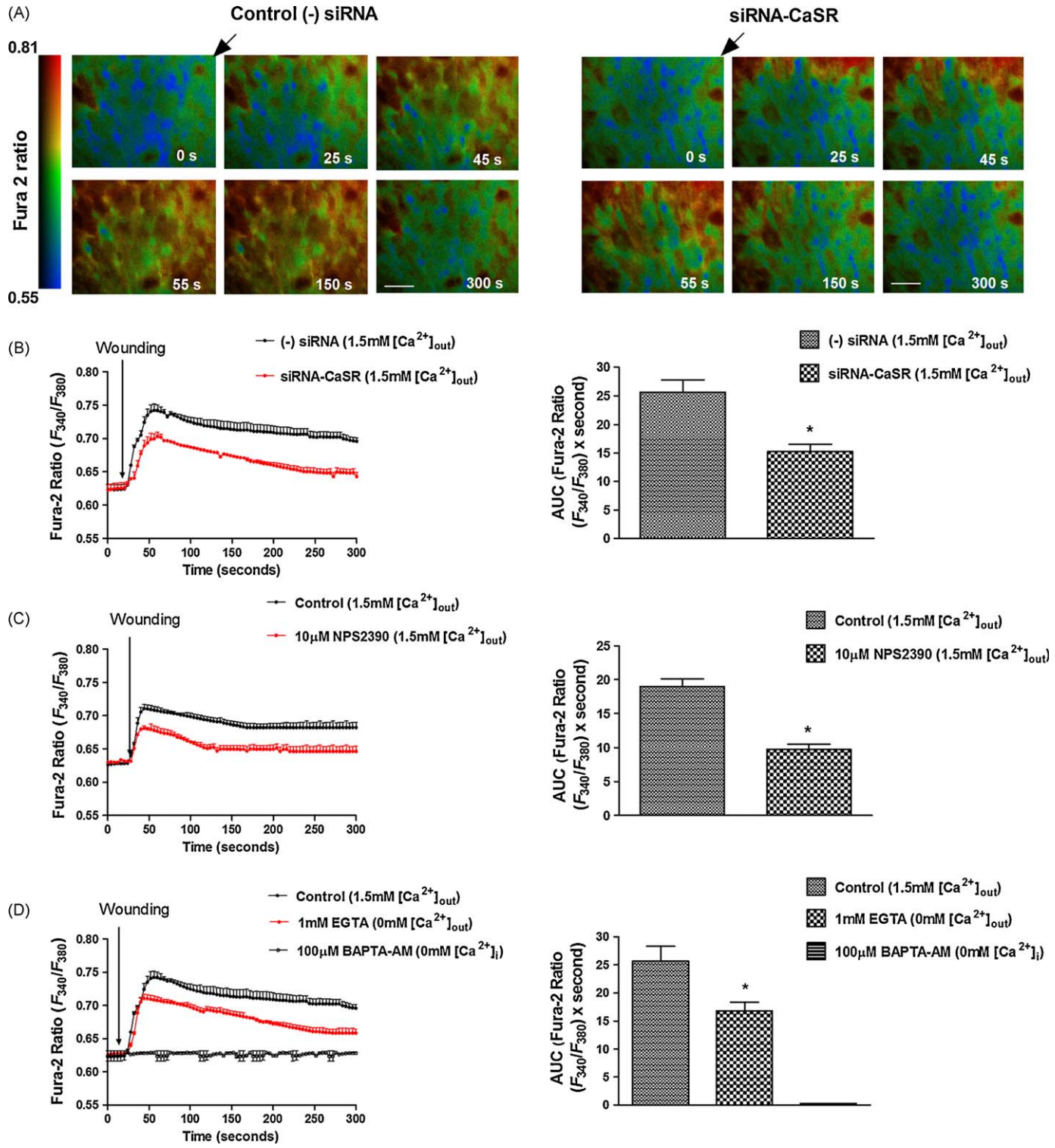

Fig. 5. Wounding produced an intracellular free Ca^{2+} concentration wave that is partially mediated by CaSR. Differentiated HBEC cultured in air-liquid interface were loaded with fura 2AM as describe above. Wounds were made in differentiated HBEC by scratching with an 18-gauge needle under various conditions. Panel (A) Representative images of Ca^{2+} waves on differentiated HBEC following wounding (black arrows) in cells transfected with (−) siRNA control (left) or with siRNA-CaSR (right). Scale bar: 50 μm. Panel (B) Differentiated HBEC transfected with (−) siRNA control (left) or with siRNA-CaSR in HBSS medium with 1.5 mM of extracellular Ca^{2+} ($[Ca^{2+}]_{out}$). Panel (C) Differentiated HBEC pretreated with or without CaSR antagonist NPS2390 in HBSS medium with 1.5 mM of $[Ca^{2+}]_{out}$. Panel (D) Differentiated HBEC pretreated with or without $[Ca^{2+}]_{out}$ chelator EGTA or intracellular Ca^{2+} ($[Ca^{2+}]_i$) chelator BAPTA-AM. Graphs are traces of the fura 2 fluorescence intensity ratio (F_{340}/F_{380}) vs. time and area under curve (AUC) of the fura 2 fluorescence ratio ((F_{340}/F_{380}) in 300 s of fluorescence measurement. Data is the mean ± SEM of 5 different experiments per condition. $^{*}P < 0.05$ vs. control.

expressed in non-differentiated and differentiated HBEC as we previously observed [14]. Whether there is a different pattern of CaSR expression between species seems to be a question to study in future works.

Previous reports have shown that CaSR activation promotes cell migration in breast cancer cells [20], osteoblasts [34] and monocytes [35] in response to elevated $[Ca^{2+}]_{out}$ similarly to that found at sites of injury or infection. In this sense, cells have levels of

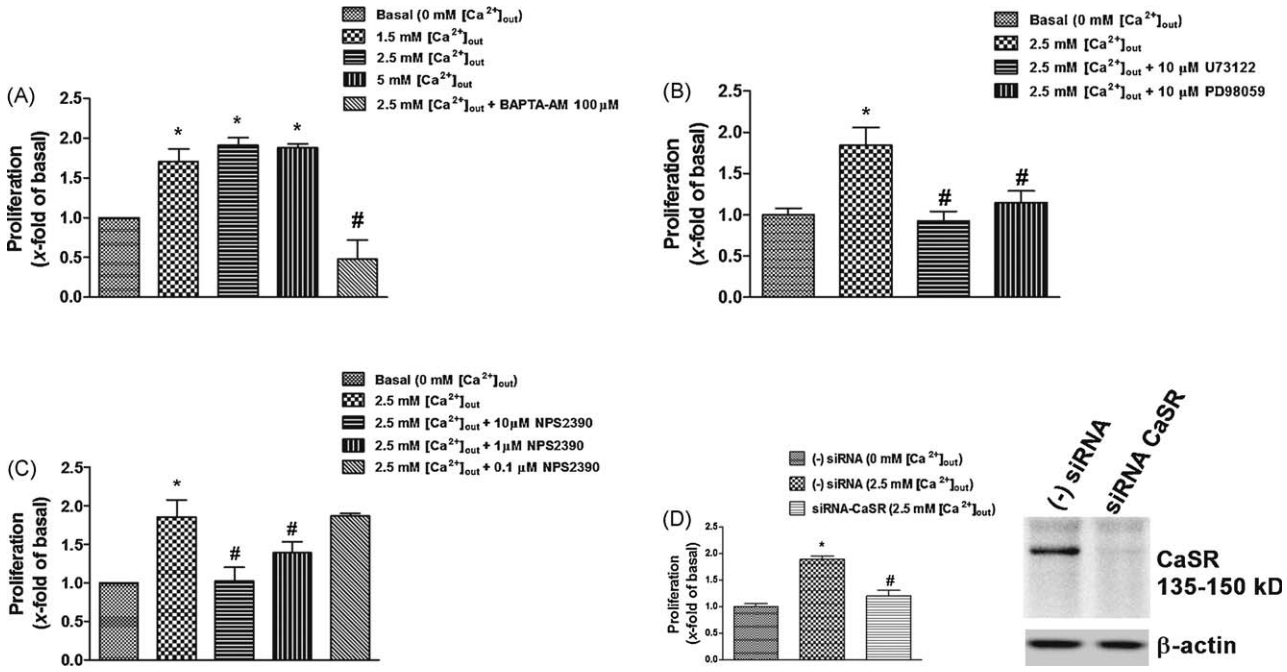

Fig. 6. Proliferation of HBEC is dependent of extracellular Ca^{2+}, PLC, ERK1/2 and CaSR. Semiconfluent HBEC were grown in presence or absence of growing extracellular Ca^{2+} concentrations ($[Ca^{2+}]_{out}$) or in presence of intracellular Ca^{2+} chelator BAPTA-AM (panel A), PLC inhibitor U73122, or the ERK1/2 inhibitor PD98059 (panel B), CaSR antagonist NPS2390 at different doses (panel C). Panel (D) shows the specific siRNA targeted to CaSR that effectively suppressed CaSR protein expression in HBEC monolayer (panel B). Then HBEC monolayer were transfect with (−) siRNA control or with siRNA-CaSR. HBEC proliferation was evaluated by the BrdU assay for 24 h as described under Section 2. Values are expressed as *x*-fold stimulation of BrdU incorporation over basal ($x = 1$). Data are mean ± SEM of 8 determinations and are representative of at least three independent experiments. $^{*}P < 0.05$ from 0 mM $[Ca^{2+}]_{out}$ medium; $^{\#}P < 0.05$ from 2.5 mM $[Ca^{2+}]_{out}$ medium.

total intracellular calcium that are substantially higher than that in the blood owing to the presence of high concentrations of calcium within intracellular stores such as endoplasmic reticulum and secretory vesicles [36]. Therefore, death or injury of cells and release of cellular calcium in a soluble form could lead to substantial local increases in $[Ca^{2+}]_{out}$. Thus we hypothesized that the high expression of CaSR on bronchial epithelial cells could be related with epithelial cell migration and repair in response to lung injury, where $[Ca^{2+}]_{out}$, which is its natural agonist, are highly increased. In this sense, we observed that increasing $[Ca^{2+}]_{out}$ induced $[Ca^{2+}]_i$ and migration of differentiated HBEC which was partially reversed by the inhibition of PLC, ERK1/2 and by the suppression of $[Ca^{2+}]_{out}$ or $[Ca^{2+}]_i$. Furthermore, simultaneously suppression of both, $[Ca^{2+}]_{out}$ and $[Ca^{2+}]_i$ completely blocked wound repair suggesting that wounding repair is totally dependent of calcium signalling. It is well known that the CaSR activation increases $[Ca^{2+}]_i$ through PLC/$InsP_3$ and phosphorylates ERK1/2 [12]. Furthermore both $[Ca^{2+}]_i$ and ERK1/2 mediate, almost in part, cell migration and wound repair [18,37]. We observed that $[Ca^{2+}]_{out}$ addition induces a dose-dependent ERK1/2 phosphorylation which was suppressed by the CaSR antagonism and by CaSR RNA silencing as previously reported in breast cancer cells [20]. These results were translated in wound repair since antagonism of CaSR and CaSR silencing also delayed wound repair.

In the process of airway epithelial repair and regeneration, migration of the basal cells neighbouring the wound is considered the first step of wound repair. However, it has been demonstrated recently that the early rapid restoration of the bronchiolar epithelium after bronchial injury is mediated by spreading and squamous metaplasia of ciliated cells, which maintain the epithelial barrier during repair [38]. In this work we have observed that CaSR is expressed among pseudostratified bronchial epithelium. In concrete, when immunofluorescence analysis was performed after 24 h post-wound CaSR was expressed on cells neighbouring the wound. Furthermore, squamous cells and ciliated cell showed a high CaSR expression at different distances of the wound which may be related with the role of CaSR on wound repair studied in this work. But the mechanism underlying CaSR-induced wound repair can become even more complicated since CaSR may transactivate epidermal growth factor receptor (EGFR) and its downstream MAPK cascade [39] promoting cell migration and proliferation.

Following cell migration, proliferation and active mitosis are the subsequent steps in the global process of wound repair. At this respect, we have observed that $[Ca^{2+}]_{out}$ activates HBEC proliferation by means of CaSR, since its inhibition and specific RNA silencing partially suppress this effect. Furthermore HBEC proliferation was suppressed by the inhibition of PLC and ERK1/2. Previously it has been shown that CaSR mediates cell proliferation in breast cancer cells [40], rat aortic vascular smooth muscle cells [24], mouse mesangial cells [41] and osteoblasts among other [34] which is in line with our results.

But one of the most interesting functions of CaSR related with wound repair seems to be the capacity to mediate the communication between cells. In this mechanism, cellular damage induces a $[Ca^{2+}]_i$ wave signal that is propagated between cells. This propagation is partially mediated by gap junctions [42,43] and mechanisms that involve the release of cellular ATP to the extracellular space with concomitant stimulation of purinergic receptors on neighbouring cells [4]. But another system that allows $[Ca^{2+}]_i$ wave propagation implicates CaSR. Here, cell damage releases $[Ca^{2+}]_{out}$ that specifically activates CaSR on neighbouring cells which express it. Thus, CaSR activation releases intracellular stores of Ca^{2+} through PLC/InP_3 which is invariably accompanied by Ca^{2+} influx across the plasma membrane to the intercellular space microenvironment. Ca^{2+} extrusion may be mediated by the plasma-membrane Ca^{2+} ATPase, Na^+/Ca^{2+} exchange, voltage-operated and store operated Ca^{2+} channels and through exocytosis of secretory granules, which again can activate CaSR located on the adjacent cells as it has been demonstrated previously in HEK-CaSR cell constructs [10,25]. In this work, we studied the role of CaSR in

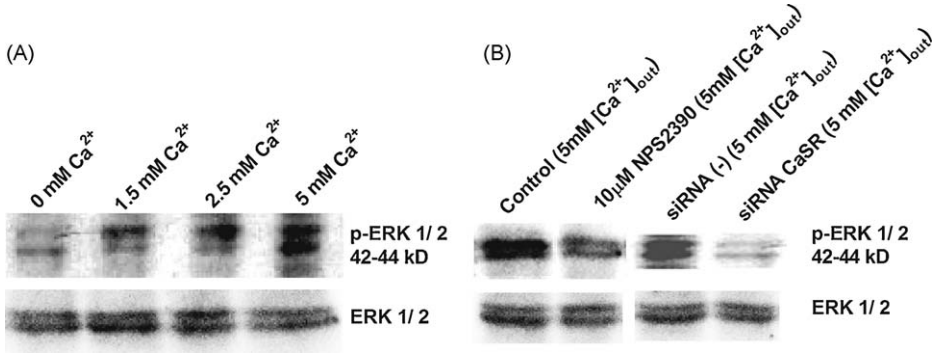

Fig. 7. Extracellular Ca^{2+} activates ERK1/2 through CaSR in differentiated HBEC. Panel (A) Western blot analysis of phosphor-ERK1/2 following different extracellular Ca^{2+} ($[Ca^{2+}]_{out}$) concentrations stimulations in a period of 20 min in differentiated HBEC. Panel (B) ERK1/2 activation in NPS2390 treated cells or in siRNA-CaSR and control (−) siRNA transfected HBEC in response to $[Ca^{2+}]_{out}$. A reduction in the $[Ca^{2+}]_{out}$-induced increase in ERK1/2 phosphorylation was observed in NPS2390 and and siRNA-CaSR transfected cells, implicating the CaSR in the effect. The results are representative of at least 3 experiments.

cell–cell communication after mechanical injury of well-differentiated HBEC. Both, protein silencing and antagonism of CaSR resulted in a diminished $[Ca^{2+}]_i$ wave propagation. Furthermore, removal of the $[Ca^{2+}]_{out}$ with EGTA also reduced $[Ca^{2+}]_i$ wave propagation by uncoupling $[Ca^{2+}]_i$–$[Ca^{2+}]_{out}$ cycle as previously was shown in different wounding cellular models [6,17].

Repair of the airway epithelium after injury is critical for the maintenance of the barrier function and the limitation of airway hyperreactivity. Improving our understanding of epithelial function in normal and pathologic conditions, through *in vitro* models that mimic human airway epithelial injury repair and regeneration, may help to develop novel regenerative therapeutics allowing the rapid repair and regeneration of a functional airway epithelium in lung disorders such as COPD or asthma.

5. Conclusions

The present study provides cellular evidence that CaSR actively participates in the repair of the bronchus epithelium after acute injury through rapid cell migration and posterior proliferation of HBEC. In this process CaSR activation promotes cell–cell communication through $[Ca^{2+}]_i$ wave propagation which may be translated in a novel type of intercellular communication in the human airway epithelium.

Conflict of interest

The authors declare that they do not have any actual or potential conflict of interest including any financial, personal or other relationships with other people or organizations within three years of beginning this submitted work that could inappropriately influence, or be perceived to influence, our work.

Acknowledgements

This work was supported by grants SAF2005-00669/SAF2008-03113 (JC), SAF2006-01002/SAF2009-08913 (EJM), CIBERES (CB06/06/0027) and CAIBER (CAI08/01/0039) from Ministry of Science and Innovation and Health Institute 'Carlos III' of Spanish Government, and research grants from Regional Government (Prometeo/2008/045; 'Generalitat Valenciana'). JM has a research contract from 'Fondo de Investigaciones Sanitarias' (FIS) of Health Institute 'Carlos III' of Ministry of Health (Spain).

References

[1] Laitinen LA, Heino M, Laitinen A, Kava T, Haahtela T. Damage of the airway epithelium and bronchial reactivity in patients with asthma. Am Rev Respir Dis 1985;131:599–606.
[2] Puchelle E, Zahm JM, Tournier JM, Coraux C. Airway epithelial repair, regeneration, and remodeling after injury in chronic obstructive pulmonary disease. Proc Am Thorac Soc 2006;3:726–33.
[3] McDowell EM, Becci PJ, Schurch W, Trump BF. The respiratory epithelium. VII. Epidermoid metaplasia of hamster tracheal epithelium during regeneration following mechanical injury. J Natl Cancer Inst 1979;62:995–1008.
[4] Isakson BE, Evans WH, Boitano S. Intercellular Ca^{2+} signaling in alveolar epithelial cells through gap junctions and by extracellular ATP. Am J Physiol Lung Cell Mol Physiol 2001;280:L221–8.
[5] Isakson BE, Seedorf GJ, Lubman RL, Evans WH, Boitano S. Cell–cell communication in heterocellular cultures of alveolar epithelial cells. Am J Respir Cell Mol Biol 2003;29:552–61.
[6] Hinman LE, Beilman GJ, Groehler KE, Sammak PJ. Wound-induced calcium waves in alveolar type II cells. Am J Physiol 1997;273:L1242–8.
[7] Camello P, Gardner J, Petersen OH, Tepikin AV. Calcium dependence of calcium extrusion and calcium uptake in mouse pancreatic acinar cells. J Physiol 1996;490(Pt 3):585–93.
[8] Yamoah EN, Lumpkin EA, Dumont RA, Smith PJ, Hudspeth AJ, Gillespie PG. Plasma membrane Ca^{2+}-ATPase extrudes Ca^{2+} from hair cell stereocilia. J Neurosci 1998;18:610–24.
[9] Berridge MJ, Bootman MD, Roderick HL. Calcium signalling: dynamics, homeostasis and remodelling. Nat Rev Mol Cell Biol 2003;4:517–29.
[10] Hofer AM, Curci S, Doble MA, Brown EM, Soybel DI. Intercellular communication mediated by the extracellular calcium-sensing receptor. Nat Cell Biol 2000;2:392–8.
[11] Brown EM, MacLeod RJ. Extracellular calcium sensing and extracellular calcium signaling. Physiol Rev 2001;81:239–97.
[12] Ward DT. Calcium receptor-mediated intracellular signalling. Cell Calcium 2004;35:217–28.
[13] Ruat M, Molliver ME, Snowman AM, Snyder SH. Calcium sensing receptor: molecular cloning in rat and localization to nerve terminals. Proc Natl Acad Sci USA 1995;92:3161–5.
[14] Cortijo J, Milara J, Mata M, Donet E, Gavara N, Peel SE, et al. Nickel induces intracellular calcium mobilization and pathophysiological responses in human cultured airway epithelial cells. Chem Biol Interact 2009.
[15] Cortijo J, Marti-Cabrera M, de la Asuncion JG, Pallardo FV, Esteras A, Bruseghini L, et al. Contraction of human airways by oxidative stress protection by N-acetylcysteine. Free Radic Biol Med 1999;27:392–400.
[16] Dalli E, Milara J, Cortijo J, Morcillo EJ, Cosin-Sales J, Sotillo JF. Hawthorn extract inhibits human isolated neutrophil functions. Pharmacol Res 2008;57:445–50.
[17] Sammak PJ, Hinman LE, Tran PO, Sjaastad MD, Machen TE. How do injured cells communicate with the surviving cell monolayer? J Cell Sci 1997;110(Pt 4):465–75.
[18] Wadsworth SJ, Nijmeh HS, Hall IP. Glucocorticoids increase repair potential in a novel in vitro human airway epithelial wounding model. J Clin Immunol 2006;26:376–87.
[19] Corteling RL, Brett SE, Yin H, Zheng XL, Walsh MP, Welsh DG. The functional consequence of RhoA knockdown by RNA interference in rat cerebral arteries. Am J Physiol Heart Circ Physiol 2007;293:H440–7.
[20] Saidak Z, Boudot C, Abdoune R, Petit L, Brazier M, Mentaverri R, et al. Extracellular calcium promotes the migration of breast cancer cells through the activation of the calcium sensing receptor. Exp Cell Res 2009;315:2072–80.
[21] Wei C, Wang X, Chen M, Ouyang K, Song LS, Cheng H. Calcium flickers steer cell migration. Nature 2009;457:901–5.
[22] Cifuentes M, Rojas CV. Antilipolytic effect of calcium-sensing receptor in human adipocytes. Mol Cell Biochem 2008;319:17–21.
[23] Hammond CM, White D, Tomic J, Shi Y, Spaner DE. Extracellular calcium sensing promotes human B-cell activation and function. Blood 2007;110:3985–95.
[24] Smajilovic S, Hansen JL, Christoffersen TE, Lewin E, Sheikh SP, Terwilliger EF, et al. Extracellular calcium sensing in rat aortic vascular smooth muscle cells. Biochem Biophys Res Commun 2006;348:1215–23.

[25] Hofer AM, Gerbino A, Caroppo R, Curci S. The extracellular calcium-sensing receptor and cell–cell signaling in epithelia. Cell Calcium 2004;35:297–306.
[26] Brown EM, Gamba G, Riccardi D, Lombardi M, Butters R, Kifor O, et al. Cloning and characterization of an extracellular Ca(2+)-sensing receptor from bovine parathyroid. Nature 1993;366:575–80.
[27] Geibel JP, Hebert SC. The functions and roles of the extracellular Ca^{2+}-sensing receptor along the gastrointestinal tract. Annu Rev Physiol 2009;71: 205–17.
[28] Arabzadeh A, Troy TC, Turksen K. Insights into the role of the calcium sensing receptor in epidermal differentiation in vivo. Mol Biotechnol 2009;43:264–72.
[29] Yano S, Brown EM, Chattopadhyay N. Calcium-sensing receptor in the brain. Cell Calcium 2004;35:257–64.
[30] Rodland KD. The role of the calcium-sensing receptor in cancer. Cell Calcium 2004;35:291–5.
[31] Molostvov G, Bland R, Zehnder D. Expression and role of the calcium-sensing receptor in the blood vessel wall. Curr Pharm Biotechnol 2009;10:282–8.
[32] Yamaguchi T, Kifor O, Chattopadhyay N, Bai M, Brown EM. Extracellular calcium (Ca^{2+}o)-sensing receptor in a mouse monocyte–macrophage cell line (J774): potential mediator of the actions of Ca^{2+}o on the function of J774 cells. J Bone Miner Res 1998;13:1390–7.
[33] Finney BA, del Moral PM, Wilkinson WJ, Cayzac S, Cole M, Warburton D, et al. Regulation of mouse lung development by the extracellular calcium-sensing receptor, CaR. J Physiol 2008;586:6007–19.
[34] Yamaguchi T, Chattopadhyay N, Kifor O, Butters Jr RR, Sugimoto T, Brown EM. Mouse osteoblastic cell line (MC3T3-E1) expresses extracellular calcium (Ca^{2+}o)-sensing receptor and its agonists stimulate chemotaxis and proliferation of MC3T3-E1 cells. J Bone Miner Res 1998;13:1530–8.
[35] Olszak IT, Poznansky MC, Evans RH, Olson D, Kos C, Pollak MR, et al. Extracellular calcium elicits a chemokinetic response from monocytes in vitro and in vivo. J Clin Invest 2000;105:1299–305.
[36] Robertson WG, Marshall RW. Ionized calcium in body fluids. Crit Rev Clin Lab Sci 1981;15:85–125.
[37] Leiper LJ, Walczysko P, Kucerova R, Ou J, Shanley LJ, Lawson D, et al. The roles of calcium signaling and ERK1/2 phosphorylation in a $Pax6^{+/-}$ mouse model of epithelial wound-healing delay. BMC Biol 2006;4:27.
[38] Park KS, Wells JM, Zorn AM, Wert SE, Laubach VE, Fernandez LG, et al. Transdifferentiation of ciliated cells during repair of the respiratory epithelium. Am J Respir Cell Mol Biol 2006;34:151–7.
[39] MacLeod RJ, Yano S, Chattopadhyay N, Brown EM. Extracellular calcium-sensing receptor transactivates the epidermal growth factor receptor by a triple-membrane-spanning signaling mechanism. Biochem Biophys Res Commun 2004;320:455–60.
[40] El Hiani Y, Lehen'kyi V, Ouadid-Ahidouch H, Ahidouch A. Activation of the calcium-sensing receptor by high calcium induced breast cancer cell proliferation and TRPC1 cation channel over-expression potentially through EGFR pathways. Arch Biochem Biophys 2009;486:58–63.
[41] Kwak JO, Kwak J, Kim HW, Oh KJ, Kim YT, Jung SM, et al. The extracellular calcium sensing receptor is expressed in mouse mesangial cells and modulates cell proliferation. Exp Mol Med 2005;37:457–65.
[42] Boitano S, Dirksen ER, Sanderson MJ. Intercellular propagation of calcium waves mediated by inositol trisphosphate. Science 1992;258:292–5.
[43] Charles AC, Merrill JE, Dirksen ER, Sanderson MJ. Intercellular signaling in glial cells: calcium waves and oscillations in response to mechanical stimulation and glutamate. Neuron 1991;6:983–92.